Journal of Marine Research, 44, 149–184, 1986

Early diagenesis in bioadvective sediments: Relationships between the diagenesis of beryllium-7, sediment reworking rates, and the abundance of conveyor-belt deposit-feeders

by Donald L. Rice[1,2]

ABSTRACT

Laboratory experimentation and field sampling programs were used to examine the contribution of the conveyor-belt feeding/biodeposition activity of orbiniid polychaetes, *Scoloplos* spp., to bioturbation in intertidal sediments of Lowes Cove, Maine. Laboratory measurements of particle reworking rates were incorporated into steady-state and transient-state diagenetic models to predict subduction velocities of marker layers in incubated cores from Lowes Cove and to predict the *in situ* activity-depth profile of the radionuclide Be-7 (half-life = 53.3 d), a useful, naturally-occurring tracer of rapid mixing processes.

Incubated cores containing a complete macrofauna from the Cove were mixed bioadvectively with little random mixing (peak-broadening of the marker) detectable. The conveyor-belt activity of *Scoloplos* spp. accounted fully for particle subduction in these cores.

The Be-7 activity-depth profile of a sediment core taken from Lowes Cove was consistent with a conveyor-belt diagenetic model based upon (1) seasonal variations in the surface biodeposition rate of *Scoloplos* spp. and (2) a constant Be-7 activity at the sediment surface. Although the surface Be-7 activity in principal may be affected by seasonal changes in the rates of atmospheric deposition and dilution with radioactively dead sediment emplaced by conveyor-belt activity, such effects apparently did not dominate features of this Be-7 profile.

The control by these polychaetes of sediment turnover and incorporation of reactive chemical species across the sediment surface may explain in part why local patches with characteristic worm abundance and standing crop are maintained year to year in Lowes Cove.

1. Introduction

The physical, geochemical, and ecological development of the bioturbated zone of a sedimentary deposit is dependent upon a complex set of interacting transport phenomena, quasi-equilibrium and nonequilibrium chemical reactions, and benthic community dynamics. In all three of these aspects, the macrobenthos figure prominently as agents of physical transport and biogeochemical catalysis (Aller, 1982; Fisher, 1982). For example, the feeding and burrowing activities of the macroinfauna may not only exert major effects upon the vertical and horizontal distributions of particulates and

1. Department of Geological Sciences and Environmental Studies, State University of New York, Binghamton, New York, 13901, U.S.A.

2. Present address: Chesapeake Biological Laboratory, Center for Environmental and Estuarine Studies, University of Maryland, Solomons, Maryland, 20688, U.S.A.

interstitial fluids but may also affect the standing crop, community composition, and physiological state of the benthic microflora, which in turn exert major controls upon the biogeochemistry of the deposit. Because of this intimate relationship between the macrobenthos and the physical and biogeochemical state of the deposit, it is clear that the intensity and spatial distribution of their effect is dependent upon both the composition of the macrofaunal community and the density of constituent populations.

The importance of the macrobenthos in sediment mixing is well established. Recognition of the usefulness of particle-reactive radionuclides such as Pb-210 and Cs-137 in quantifying relatively long-term (years to decades) mixing (Robbins *et al.*, 1977; Nozaki *et al.*, 1977) and the use of Th-234 and Be-7 to evaluate rapid (on the order of weeks to months) mixing processes (Aller and Cochran, 1976; Krishnaswami *et al.*, 1980) have facilitated the study of diagenetic reaction kinetics in the bioturbated zone. The theoretical basis normally used to interpret the radioisotope data (Goldberg and Koide, 1962) assumes that mixing is spatially random and, therefore, quantifiable as an eddy diffusive process (Guinasso and Schink, 1975). Although the assumption of random mixing is generally an oversimplification of reality in many sediments, the eddy diffusive model is a convenient fiction because of the mathematical elegance of the solutions to the types of reaction-transport diagenetic equations commonly employed.

Macroinfauna which feed at depth and egest particles upon the sediment surface ("conveyor-belt feeders" *sensu* Rhoads (1974)) contribute an important non-random bioadvective component to sediment mixing and are potentially the principal agents in bioturbation. Conveyor-belt feeders are typically polychaetous annelids, but the distinction extends to several invertebrate taxa containing vermiform representatives (e.g., hemichordates, holothurians, estuarine oligochaetes). In marine environments, the conveyor-belt feeding habit is characteristic of mid- to late-stage benthic community succession, the feeding activity occurring commonly in the vicinity of the redox potential discontinuity (RPD) (Rhoads, 1974; Rhoads and Boyer, 1982). Populations of such species may transport enormous quantities of particulates over a vertical distance of several centimeters yearly (Rhoads, 1974; McCall and Tevesz, 1982). In a series of elegant experimental studies in freshwater sediments, Robbins and his coworkers demonstrated that sediments dominated by subsurface-feeding tubificid oligochaetes were mixed bioadvectively; the random contribution to mixing ("peak broadening") was far less important (Robbins *et al.*, 1979; Fisher *et al.*, 1980). Some amphipods such as *Corophium volutator* and *Pontoporeia affinis,* which live in the top 1–2 cm of marine and freshwater sediments respectively, probably do contribute a strong random component to mixing when they are present at sufficiently high densities (Robbins *et al.*, 1979). In contrast, macrofauna which contribute to mixing by burrowing alone probably do little more than move particles a few millimeters to the side to permit passage of the body; the material so moved may recover viscoelastically

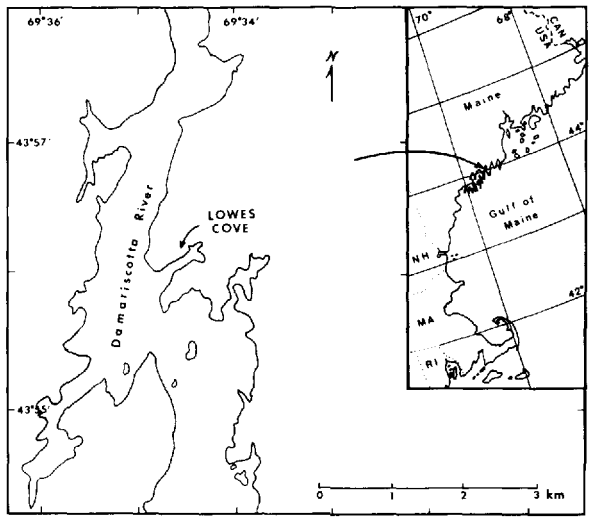

Figure 1. Damariscotta region of the coast of Maine showing the location of Lowes Cove.

to near its original position after the burrower has moved away (McCall and Tevesz, 1982). Because populations of conveyor-belt feeders have the inherent capacity to move sediment over relatively large distances in short periods of time, one might postulate that such populations dominate bioturbation in sediments inhabited by mid- to late-stage benthic communities.

Over the past three years, we have studied early diagenetic processes in an intertidal environment characterized by patchy distributions of conveyor-belt feeding orbiniid polychaetes, *Scoloplos* spp. Characteristic densities of *Scoloplos* are maintained on both a seasonal and an annual basis at specific subregions within the study area, thus affording an opportunity to assess how different levels of bioadvective transport are related to the overall mixing process, early diagenetic changes, and population density-dependent feedback mechanisms. In this paper, we report the results of laboratory and field studies of relationships between the standing crop of *Scoloplos* and the overall transport properties of the sedimentary deposit, including vertical advective velocities and the activity-depth profile of the relatively short-lived (half-life = 53.3 days), naturally-occurring radioisotope beryllium-7.

a. Study area. The field portion of this research was carried out between August, 1981 and June, 1984 in Lowes Cove, Maine, a tidal flat on the eastern margin of the Damariscotta River estuary (Fig. 1). Near its mouth, the Cove is separated from surrounding forest by rock outcrops which are colonized along their lower extremities by the fucoid macroalgae *Ascophyllum nodosum* (the dominant) and *Fucus vesiculosus*. The inner Cove is fringed by a narrow (0–7 m) embankment of the marshgrasses

Spartina alterniflora (bank edges) and *Spartina patens* (upper intertidal), within which there are local thick patches of *Ascophyllum nodusum* var. *scorpioides* and several species of minor salt marsh plants. On an average high tide, water depth at the mouth is ca. 3–4 m and at the head is ca. 1–2 m.

The tidal flat is a chemically heterogeneous and physically dynamic sedimentation basin. The sediment is a sandy clayey silt containing approximately 65% quartz, 5% chlorite and other phyllosilicates, and 20% other silicates by weight; the remainder is principally calcium carbonate (predominately calcite) and 2–6% organic matter. Anderson *et al.* (1981) have determined an average surface sedimentation rate for the Cove of 0.9 cm · y^{-1}, which is in fair agreement with our own estimates of 0.8–1.2 cm · y^{-1} based upon Pb-210 and Cs-137 depth distributions (our unpublished data) below the bioturbated zone corrected for surface porosity with the steady-state compaction equation (see Berner, 1980). Although the flat is overall an accretionary environment, most areas undergo successive erosional and depositional events throughout the year; consequently, surface sediment is continuously redistributed horizontally as positive relief features erode and depressions fill in (Anderson *et al.*, 1981).

b. Macrobenthos. The most common members of the Lowes Cove macrofauna are shown in Figure 2. In some cases, the taxonomic affinities of the organisms are only imperfectly known (e.g., the oligochaetes, which are difficult to identify).

By virtue of their suspension feeding activities, the bivalve molluscs *Macoma balthica, Mya arenaria,* and *Mytilus edulis* are major contributors to sediment accumulation (Anderson *et al.*, 1981). *Macoma* is also a vigorous surface deposit-feeder. *Macoma* (at densities of a few hundred · m^{-2}) and *Mya* (0 to 200 · m^{-2}) are distributed throughout the study area. *Mytilus* forms a very prominent reef several meters wide extending across the mouth of the Cove. Biodeposition and hydraulic baffling by these mussels has created a distinct mound of sediment which flanks the reef on both sides; the sediment in the vicinity of the mussel reef in markedly thicker, has a higher water content, and supports a richer deposit-feeding fauna than sediment in the upper Cove. Although littorinid gastropods occur in large numbers along the rocky margins of the flat, especially in association with macroalgal stands, the only gastropod commonly found on the flat is the small surface grazer *Hydrobia totteni,* which occurs in densities of 0 · m^{-2} in the lower intertidal to more than 20,000 · m^{-2} in the upper intertidal zone (unpublished data).

A wide variety of polychaetes inhabit these sediments. *Nereis succinea* (densities of 100–600 · m^{-2}), a surface-feeding omnivore that lives in a more or less permanent tube, and small suspension- and surface deposit-feeding polychaetes of the families Spionidae (principally *Strebospio benedicti* and *Polydora ligni*) and Cirratulidae (principally *Tharyx acutus*) (densities ranging from several hundred to more than 4000 · m^{-2}) are found throughout the flat. The two other ubiquitous polychaete taxa are the capitellid *Heteromastus filiformis* (typically 10–300 · m^{-2}) and several species

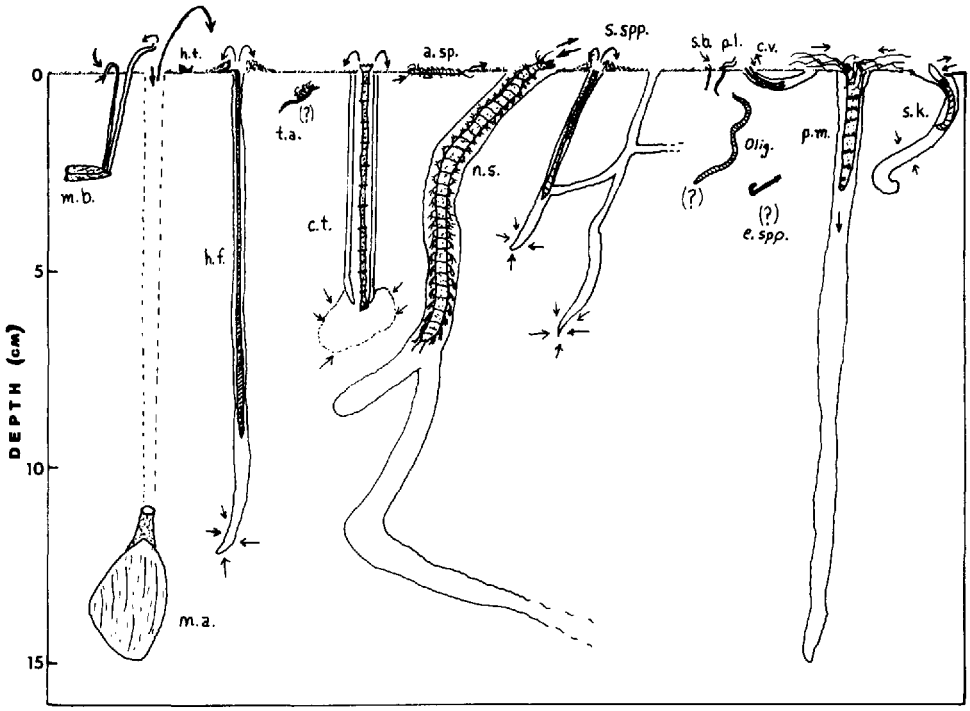

Figure 2. Macrobenthos of Lowes Cove sampling stations monitored from August, 1981, through July, 1984. Abundant taxa are shown along with major modes of particle transport (arrows) associated with each. Vertical scale is accurate; horizontal scale is exaggerated. Fauna (left to right) are: *Macoma balthica, Mya arenaria, Hydrobia totteni, Heteromastus filiformis, Tharyx acutus, Clymenella torquata, Aglaophamus* sp., *Nereis succinea, Scoloplos* spp., *Streblospio benedicti, Polydora ligni,* various oligochaetes, *Corophium volutator, Eteone* spp., *Polycirrus medusa,* and *Saccoglossus kowalewskii.*

of the orbiniid genus *Scoloplos* (200–3000+ · m^{-2}). *Heteromastus* and *Scoloplos* spp. are typical conveyor-belt deposit-feeders, the former feeding typically at a depth of 12–16 cm and the latter at 4–6 cm (the position of the RPD). Another conveyor-belt feeder, the maldanid *Clymenella torquata,* is found in isolated patches in coarse sand along the northern flank of the Cove. A surface grazer, *Aglaophamus* sp. (Nephtyidae), which apparently feeds by skimming the sediment surface, and a tentaculate surface deposit-feeder, *Polycirrus medusa* (Terebellidae), are common during summer months on the flanks of the mussel reef.

Other species which occur in locally dense patches include *Eteone* spp. (Phyllodocidae: Polychaeta); the acorn worm, *Saccoglossus kowalewskii* (Harrimanidae: Hemichordata); and several species of oligochaetes. During warmer months, the amphipod *Corophium volutator,* a vigorous mixer of the top 1–2 cm of sediment, may be found in some headward regions of the Cove at densities approaching 4000 individuals · m^{-2}.

The orbiniid polychaetes *Scoloplos* spp. are of particular interest for present purposes. We have found individuals of this genus in every core we have taken from Lowes Cove for the past four years. The average standing biomass of *Scoloplos* spp. in the Cove is 1600 mg dry wt. · m^{-2}; the typical abundance is 1000–2000 individuals · m^{-2}. It is clearly the most widely distributed abundant conveyor-belt feeder in the silty sediments constituting most of the floor of Lowes Cove, and it also occurs in coarser sandy deposits along the Cove margins where it appears to compete successfully for subsurface food resources with highly localized patches of *Clymenella torquata*. The only other conveyor-belt feeder occurring throughout the Cove, *Heteromastus filiformis*, is much less abundant. Populations of *Scoloplos fragilis* may also flourish in higher energy, sandy environments (Meyers, 1977a,b; Brown, 1982). The genus has a well-deserved reputation as a "ubiquitous" taxon capable of surviving in a variety of sedimentary environments (Johnson, 1971).

Four species of Scoloplos have been identified in Lowes Cove to date: *S. robustus*, *S. acutus*, *S. fragilis*, and *S. armiger* (L. Watling and A. Hillyard, personal communication). Except for the small size of *S. armiger*, these species differ morphologically only in fine anatomic detail; all are conveyor-belt feeders and, in laboratory cultures and incubated cores from the field, ingest particles preferentially near the RPD (4–6 cm in Lowes Cove). These worms produce surface biodeposits of high porosity (82 ± 2%). *Scoloplos* spp. burrows are subvertical, temporary structures without distinct walls and collapse within a few days after abandonment. For reasons unknown to us, these worms occasionally burrow into deep anoxic sediment (10–15 cm) where they may remain motionless, without feeding and without contact with oxygenated water, for up to two weeks; afterward they return to the top 4–6 cm, invert themselves, and resume normal feeding activity. In our work from 1981 through 1983, we have found that *S. robustus* accounts for the great majority (74%) of the individuals identified to the species level with *S. fragilis* and *S. Acutus* in about equal numbers accounting for the remainder. We have not found *S. armiger* in our samples, possibly because our sediment sieve size (500 μm) would not retain *S. armiger*.

2. Methods

a. Temporal and spatial distribution of macrofauna. The Lowes Cove benthic macrofaunal community at three stations designated 6, 7, and 8 was sampled 6 to 7 times from August, 1981, to June, 1983 (Fig. 3). These stations were selected for detailed study after a more extensive reconnaissance of the Cove because of similarities in macrofaunal species and numbers, except for differences in abundance of *Scoloplos* spp. Stations 6, 7, and 8 respectively represent very low, slightly less than average, and very high density patches of this polychaete (see Fig. 4 below). A fourth station, 84-6, was established in June, 1984, on the basis of previous records as a site with a more average *Scoloplos* patch density. Cylindrical box cores (15.2 cm diameter × 20 to 30 cm depth) were taken manually in August, 1981; March, June, August, and

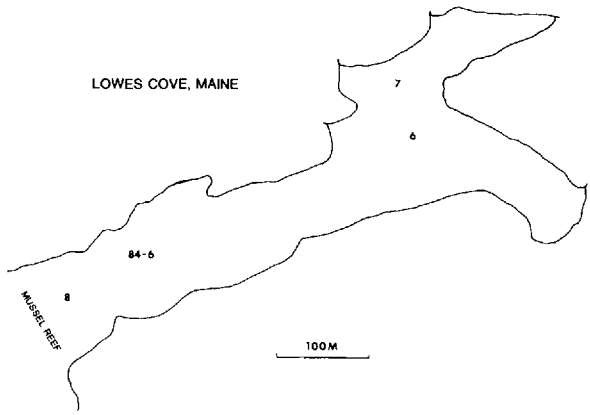

Figure 3. Location of Lowes Cove sampling stations monitored from August, 1980, through July, 1984.

November, 1982; and in April and June of 1983. Triplicate cores were taken at each station during the initial sampling, and duplicates were taken during the 1982 and 1983 samplings.

Living macrofauna were isolated by gentle wet-sieving through a 500 μm mesh polyethylene sieve, identified, and counted. *Scoloplos* spp. were allowed to stand in seawater for several hours without sediment to permit as much clearance of ingested particulates from the gut as possible; they were then dried at 80°C and weighed to calculate standing crop. Because *Scoloplos* specimens were usually destined for trace element assay, no attempt was made to carry them through the common chemical staining and killing procedures necessary for positive identification to species level.

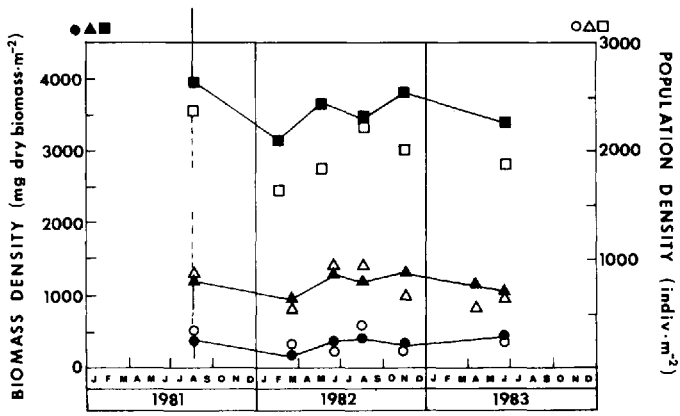

Figure 4. Biomass and abundance of *Scoloplos* spp. in Lowes Cove, August, 1981–June, 1983. Biomass (dark symbols) and number (light symbols) densities are shown for stations 6 (●, ○), 7 (▲, △), and 8 (■, □). One tail of the standard deviations from averages of three cores at each station is given for each August, 1981, datum.

b. Biodeposition rates. In August, 1981, a simple laboratory experiment was performed to estimate biodeposition rates by *Scoloplos.* Sediment from the upper 5–6 cm from Lowes Cove was wet-sieved through a 500 μm mesh polyethylene sieve using a minimum amount of seawater and frozen to kill any small fauna which might have passed through the sieve. After thawing, wet sediment was placed into four small microaquaria (50 cm area × 7 cm deep) to a depth of 5 cm. After allowing the microaquaria to remain in a well-aerated, temperature-regulated (21 ± 1°C) seawater bath for 2 days, healthy *Scoloplos robustus* were added to each. After a 3-day period to permit establishment of burrows, surface mounds were leveled by gently agitating the microaquaria. After 48 hours, biodeposits from each microaquarium were collected with a pipette and placed into aluminum weighing pans. After removing the supernatant seawater from the weighing pans, the biodeposits were washed with a few ml of distilled water, dried at 110°C for 8 hr and weighed to determine deposition rates in each microaquarium. A second collection of biodeposits was made after 60 hours and carried through the same procedure. After the second collection, the worms were recovered, placed into dishes of seawater for 16 hr to purge their gut of as much sediment as possible, dried at 80°C for 6 hr, and weighed. Biodeposition rates per unit biomass were then calculated.

c. Bioadvection in incubated cores. In August, 1982, cores were taken from stations 7 and 8 for laboratory incubation studies of sediment reworking. One core was taken at each of two sites within 4 m of the sampling sites of August, 1981, using the same types of corers as before. The incubation core from Station 7 (designated core C-7) was 16 cm deep; the core from Station 8 (designated core C-8) was 19 cm deep. Both cores were capped on the bottom and transported to the laboratory where they were immersed in a tank of well-aerated seawater and allowed to acclimate for two weeks. After acclimation, the reworking experiment itself was begun. A modification of the method of Aller and Dodge (1974) was used. Surface mounds were leveled by gentle agitation of the supernatant water, and a thin (ca. 1 mm) marker layer composed of coarse quartz sand (ca. 1 mm particle diameter) and chalk dust was deposited upon the sediment surface. Cores were incubated at 21 ± 2°C for 90 days during which the supernatant water in each was manually agitated every 2–3 days to level new mounds. Every 14 days, 2 subcores were taken from each incubation core using clear thin-walled polystyrene tubing (0.7 cm diameter). After noting the depth and the width of the marker layer, sediment was carefully extruded back into place. Between day-70 and day-90, the system temperature control malfunctioned so that the seawater temperature dropped somewhat erratically to near 17°C by day 90; consequently, data from the last 20 days may be of lesser quality than the earlier data.

d. Beryllium-7 profiles. In July, 1984, cores were taken at station 84-6 for analysis of macrofaunal composition and vertical Be-7 profiles. Manually-operated, rectangular

plexiglass box corers (28 cm L × 10 cm W × 30 cm D), similar in design to those used by Aller (1980), were used to take duplicate cores for both macrofaunal and Be-7 analysis. These cores were transported to a nearby laboratory at the I. C. Darling Center for further processing within one hour after collection. Macrofaunal density and biomass were determined as described above. Cores destined for radioisotope analysis were extruded and sectioned at 0.5-cm intervals to a depth of 4 cm, followed by 1-cm intervals to 8 cm depth and 2- or 3-cm intervals to 20 cm depth. Approximately 1 cm of material was trimmed from the edge of each section to avoid contaminating deeper sections with Be-7-rich particles from shallower material adhering to box corer walls. Ancillary cores were taken for gravimetric determination of water content (dessication at 80°C) and calculation of porosites.

Be-7 was determined on bulk dry sediment samples (ca. 200–250 g) from each section by non-destructive gamma spectrometry (Larsen and Cutshall, 1981). Prior to gamma counting, shell and rock fragments were removed and concretions were manually pulverized. Samples were retained in identical Marinelli (re-entrant) geometries and counted for 12 h using a coaxial intrinsic germanium detector shielded by 20 cm of low-background (ca. 0.2 dpm in the vicinity of the Be-7 477.6 keV photopeak) mild steel. After correction for background, detector and gamma efficiencies, and time lapse between core retrieval from the field and actual radioassay, absolute *in situ* Be-7 activities were calculated using NBS radioactivity standards for calibration.

3. Results

a. Temporal and spatial variations in Scoloplos abundance. Scoloplos biomass and number densities at Stations 6, 7, and 8 were maintained at distinct levels from August, 1981, through June, 1983 (Fig. 4). Time-averaged biomass densities for these stations respectively were 342, 1171, and 3566 mg dry worm · m^{-2}, all within the range of uncertainty calculated from the triplicate sampling in August, 1981. Corresponding time-averaged number densities were 242, 736, and 1983 indiv · m^{-2}. Even without data for the winter months, it is clear that characteristic number and biomass densities were maintained at each station over the 22 month monitoring period.

b. Rates of biodeposition by Scoloplos. At 21°C, the surface biodeposition rate by *Scoloplos robustus* was 120 ± 3 mg dry sediment · mg dry biomass^{-1} · d^{-1} or 176 ± 55 mg dry sediment · worm^{-1} · d^{-1} (Table 1). Although rates determined by each of the two sampling events for each treatment agreed to within 4%, there were significant differences in biodeposition rates per individual between microcosms. No relationship between biodeposition rates per individual and faunal density was apparent. Biodeposition rates per unit biomass were not different between microcosms. Collectively, the data indicate that individual ingestion/egestion rates are proportional to biomass and

Table 1. Rates of epibenthic biodeposition by *Scoloplos robustus* in near-surface (0–6 cm) sediment from Lowes Cove, Maine. Temperature = 21 ± 1°C.

Scoloplos Abundance		Final Biomass	Biodeposition Rate	
Indiv · microcosm^{-1}	Indiv · m^{-2}	mg dry biomass · microcosm^{-1}	mg dry sed · indiv^{-1} · d^{-1}	mg dry sed · mg biomass^{-1} · d^{-1}
1	200	1.24	150.6 ± 3.8	121.4 ± 3.1
2	400	2.85	168.8 ± 2.7	118.4 ± 1.9
2	400	4.22	253.2 ± 8.3	120.0 ± 4.0
4	800	4.33	130.0 ± 2.6	120.1 ± 2.4

that population biodeposition rates might be predicted with greater certainty on the basis of standing biomass rather than population or number density.

c. Macrofauna and sediment turnover in incubated cores. At the end of the experiment, the general physical and macrobiological characteristics of incubation cores C7 and C8 were similar to those of sediments freshly taken from Lowes Cove. Porosity profiles of fresh and incubated cores were nearly identical (Table 2), indicating that any physical disruption of the core that might have occurred during transport to the laboratory had been ameliorated during incubation.

The macrofauna of the cores at the end of the experiment also compared favorably to that of fresh cores (Table 3). Three dead *M. balthica* (50% of total) were found in

Table 2. Porosity profiles of fresh and incubated (90 days) sediment cores from stations 7 and 8.

Depth Interval	Lowes Cove Stations (August, 1981)		Incubation Cores (August, 1982)	
(cm)	7	8	C7	C8
0	76 ± 2	80 ± 2	76	79
0–1	73 ± 1	80 ± 1	74	80
1–2	67 ± 1	79 ± 1	66	79
2–3	61 ± 1	78 ± 1	62	78
3–4	57 ± 1	77 ± 1	57	77
4–5	58 ± 1	76 ± 1	57	76
5–6	55 ± 1	74 ± 1	55	74
6–7	55 ± 1	74 ± 1	55	73
7–8	54 ± 1	73 ± 1	55	73
8–10	55 ± 1	72 ± 1	54	71
10–12	52 ± 1	70 ± 1	54	70
12–14	54 ± 1	68 ± 1	54	68
15–16		67 ± 1		67
16–18		67 ± 1		67
18–20		68 ± 0		67

Table 3. Macrofauna of stations 7 and 8 (both August, 1981) and 84–6 (July, 1984) and in incubated cores from stations 7 and 8 (taken August, 1982). Faunal counts in the two incubated cores (C7 and C8) were made at the end of the 90-day experiment.

Macrobenthos retained by 500 μm sieve			Station 7 *Avg. of 3 Cores	Station 7 **End of Expt. Core C7	Station 8 *Avg. of 3 Cores	Station 8 **End of Expt. Core C8	Station 84–6 ***Avg. of 2 Cores
Bivalvia	Tellinidae	*Macoma balthica*	397	164	41	110	316 ± 35
	Myacidae	*Mya arenaria*	137	0	0	0	0
	Mytilidae	*Mytilus edulis*	0	0	0	0	0
Gastropida	Hydrobiidae	*Hydrobia totteni*	3070	493	0	164	0
Polychaeta	Capitellidae	*Heteromastus filiformis*	14	110	14	219	70 ± 35
		Other capitellids	0	0	0	0	140 ± 70
	Cirratulidae	*Tharyx acutus*	0	384	0	329	4564 ± 878
	Maldanidae	*Clymenella torquata*	0	0	0	0	0
	Nephtyidae	*Aglaophamus* sp.	0	0	2713	658	667 ± 105
	Nereidae	*Nereis succinea*	103	219	192	219	316 ± 70
	Orbiniidae	*Scoloplos* spp.	850	1151	2384	2851	1931 ± 211
	Phyllodicidae	*Eteone* spp.	0	55	0	0	351 ± 70
	Spionidae	(See text)	206	1480	206	493	493 ± 256
	Terebellidae	*Polycirrus medusa*	0	0	14	0	70 ± 70
Oligochaeta	—	—	14	439	233	329	44 ± 31
Crustacea	Crangonidae	*Crangon septemspinosa*	0	0	41	0	0
Amphipoda	Corophiidae	*Corophium volutator*	0	55	0	0	0
Nemertea	Lineidae	—	7	0	0	0	0
Platyhelminthes	—	—	7	0	0	0	0
Hemichordata	Harrimaniidae	*Saccoglossus kowalewskii*	260	219	0	0	0

*Field sampling in August, 1981; **August, 1982, core sieved December, 1982, after incubation experiment; ***Field sampling July, 1984.

Family and/or genus-species not determined.

C7 at the end of the experiment, many *H. totteni* escaped from C7 (some apparently entered or grew to visible size in C8), and *Aglaophamus* may have escaped from C8. There may also have been substantial growth of spionids during incubation. *M. edulis, C. torquata,* and *C. septemspinosa* were purposely avoided during the selection of coring sites.

The numbers and biomass of *Scoloplos* spp. in the experimental cores were representative of the sites from which the cores were taken (Table 2 and Fig. 4). At the end of the experiment, C7 contained 1151 *Scoloplos* · m^{-2} or 1.2 g dry biomass · m^{-2}, and C8 contained 2851 *Scoloplos* · m^{-2} or 4.5 g dry biomass · m^{-2} (slightly less than 4 times the *Scoloplos* biomass of C7). This latter biomass is larger than any we have recorded for *Scoloplos* in Lowes Cove from 1981 through 1984 and may indicate that there was substantial growth during the experiment.

Although some dispersion of chalk from the marker layer was apparent, the dominant mode of transport in the incubation cores was advective (Fig. 5). Broadening of the marker layer became detectable on day-42 in C7 and on day-56 in C8. In C7, final marker layer thickness was 2 mm, and in C8 about 9 mm. The duplicate depth/layer thickness determinations usually showed good agreement (coincidence or overlap); however, disparity in the measurements in C8 on days 70 and 84 suggests that the originally horizontal marker layer had begun to take on a crenulated shape at depth because of lateral inhomogeneities in biogenic reworking.

Subduction of the marker layer was about 4.5 times faster in C8 than in C7. Average subduction velocities during days 0–56 were 0.16 ± 0.03 and 0.79 ± 0.05 mm · d^{-1} in C7 and C8 respectively. However, near the end of the experiment (days 84–90) subduction velocities at depth were 0.18 ± 0.02 and 0.68 ± 0.03 mm · d^{-1}. Despite the loss of temperature control (mentioned above), the similarities in initial and final velocities in C7 suggest that some factor other than reduced feeding due to the temperature drop may have contributed to the significant decrease in subduction velocity in C8. The appearance of traces of chalk in the surface sediment of C8 on day-56 confirmed that the marker layer had entered the feeding zone of *Scoloplos* (6 ± 1.5 cm for station 81-8 in August, 1981). The absence of chalk in the surface deposits of C7 indicated that the marker layer did not enter the *Scoloplos* feeding zone (5 ± 1.5 cm for station 81-7 in August, 1981).

d. Be-7 activity-depth relations. The vertical distribution of Be-7 activity at Station 84-6 showed a maximum of 4.6–4.8 dpm · g^{-1} near the sediment surface and a monotonic, roughly exponential decrease to a depth of 3–3.5 cm where it was not detected (Table 4). Similar profiles for this isotope have been reported for other shallow-water sediments (Krishnaswami *et al.*, 1980; Krishnaswami *et al.*, 1984). The similarity of Be-7 activities in the "surface" and 0–0.5 cm samples may indicate that the top 0.5 cm at this station is rapidly mixed on a time scale much less than the half-life of Be-7 (53.3 d), although the possibility of sampling artifacts because of our

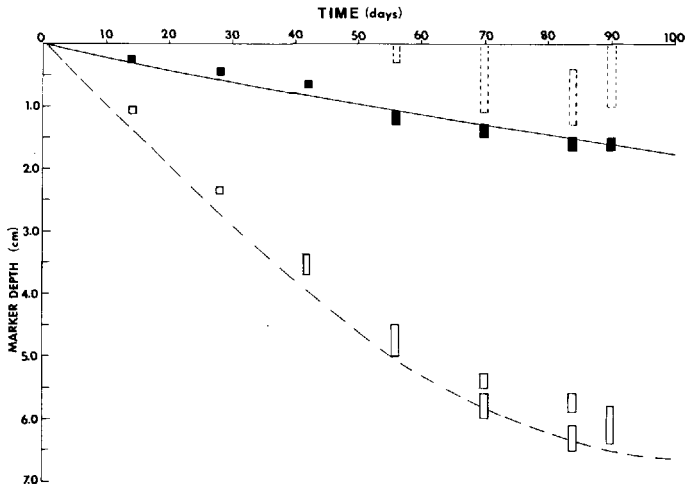

Figure 5. Subduction of marker horizons in cores C7 (dark symbols) and C8 (light symbols) during laboratory incubation at 21°C. Symbols indicate depth and thickness of marker layer. Double symbols on days 70 and 84 (core C8) indicate that duplicate determinations showed neither coincidence nor overlap; broken light symbols near surface (days 56–90) indicate diffuse distribution of marker material was found near sediment surface. Curves are theoretical predictions based upon *Scoloplos* biodeposition rate at 21°C and Eq. 13.

surface scraping technique cannot be altogether dismissed. Two localized but significant Be-7 peaks were found at depths of 7–8 cm and 10–12 cm and probably reflect direct transport of surface material to depth by avalanching or by the surface grazing activities of the polychaetes *Nereis succinea* and *Polycirrus medusa,* which have burrows that may terminate or bend sharply in this depth range.

Table 4. Be-7 activity and porosity depth variations at station 84–6 (August, 1984). Be-7 are 1-sigma counting errors. Precision of porosity measurements is better than 2% of the tabulated value.

Depth Interval (cm)	Porosity (%)	Be-7 Activity (dpm · g dry sed^{-1})	Depth Interval (cm)	Porosity (%)	Be-7 Activity (dpm · g dry sed^{-1})
0*	80	4.62 ± 0.38	4–5	64	0 ± 0.12
0.0–0.5	80	4.76 ± 0.38	5–6	64	0 ± 0.11
0.5–1.0	72	3.08 ± 0.30	6–7	62	0 ± 0.12
1.0–1.5	70	2.16 ± 0.28	7–8	62	0.78 ± 0.28
1.5–2.0	67	1.12 ± 0.25	8–10	61	0 ± 0.11
2.0–2.5	66	0.35 ± 0.22	10–12	60	0.67 ± 0.26
2.5–3.0	64	0.15 ± 0.21	12–15	58	0 ± 0.12
3.0–3.5	63	0 ± 0.12	15–20	58	0 ± 0.11
3.5–4.0	62	0.04 ± 0.19			

*Approximated by counting a thin layer of material scraped from sediment surface.

Except for the large number of cirratulids (which were also found at other stations in summer, 1984), the macrofaunal assemblage at station 84-6 in July, 1984, was typical of the central portion of Lowes Cove (Table 3). *Scoloplos* density was 1931 ± 211 individuals · m^{-2} or 1.85 ± 0.45 g dry biomass · m^{-2}, slightly higher than the average values we expected on the basis of earlier records.

4. Discussion

a. Biodeposition rates. The biodeposition rate of 120 g dry sediment · g dry worm $^{-1}$ · d^{-1} reported here (Table 1) for *Scoloplos robustus* is a rate depending upon the set of experimental control parameters used (McCall and Tevesz, 1982). We chose a temperature of 21°C (to represent mid-August in Lowes Cove), three population densities, and native sediment which for the most part had already been sorted *in situ* by these (and other) deposit-feeders. At 15 ± 1°C and 17 ± 2°C biodeposition rates by mixed cultures of *Scoloplos* spp. are 46 ± 2 and 64 ± 14 g · g^{-1} · d^{-1} (Rice *et al.*, 1986). Any two of these three rates may be used to calculate an apparent Arrhenius activation energy of 27.0 ± 0.4 kcal·mol^{-1}, predicting the third rate with high accuracy (see Eq. 32 below). The proportionality of rates of biodeposition by *Scoloplos* over the 15–21°C range is almost identical to that reported for *Tubifex tubifex* (Wachs, 1967). Although the Arrhenius relationship seems to work well in this range for these two annelids, it underestimates *Scoloplos* rate in the 0–6°C range where observed rates are around 15–20 g · g^{-1} · d^{-1} and are rather insensitive to temperature change. Because sediment used in this experiment was taken from the conveyor-belt zone of Lowes Cove, availability of ingestible particles should not have limited feeding/egestion rates, especially if particle size is a key selection criterion (Self and Jumars, 1978). Similarly the absence of an effect of worm abundance or standing crop upon biomass-specific feeding/egestion rate indicated that individuals were spatially situated so that feeding interferences did not occur. The lack of interference may reflect vertical as well as horizontal adjustment of feeding zones (McCall and Fisher, 1980). Under natural conditions in which *Scoloplos* and other conveyor-belt feeders are actually found, temperature variation probably exerts the major influence upon ingestion and biodeposition rate (McCall and Tevesz, 1982).

From these values of biomass-specific biodeposition rates, estimates of field reworking rates can be calculated. The rate R_o of Scoloplos biodeposit accretion on the sediment surface is

$$R_o = \frac{\overline{B}r}{\rho\,[1 - \phi_s]} \tag{1}$$

where $\overline{B}$ = *Scoloplos* standing crop (g biomass · m^{-2}), r = biomass-specific particle egestion rate (g particle · g biomass^{-1} · d^{-1}), ρ = average density of particulate material (g particle · cm^{-3} particle), and ϕ_s = porosity of the biodeposits (so that $1 - \phi_s$ = cm^3 particle · cm^{-3} wet sediment). Using $\phi_s = 0.82$ for typical *Scoloplos* mounds,

ρ = 2.7 g · cm^{-3}, and the 21°C (presumably mid-August) value of r = 120 g dry sediment · g dry biomass^{-1} · d^{-1} (Table 1), one gram of *Scoloplos* could produce about 7500 cm^3 of wet sediment $month^{-1}$; for a standing crop of 1 g dry biomass · m^{-2}, this is equivalent to a summertime subduction velocity of 0.75 cm · $month^{-1}$. Because feeding rates of deposit-feeders are strongly affected by temperature (McCall and Tevesz, 1982), year-averaged rates will be significantly lower. Correcting for temperature variation using the data of Rice *et al.* (1986) (see Fig. 9 inset), the yearly average biodeposition rate by *Scoloplos* spp. is about 60 g dry sediment · g dry biomass^{-1} · d^{-1}. Then for an average standing crop of 1.6 g *Scoloplos* · m^{-2} in Lowes Cove, the average surface subduction rate due to *Scoloplos* biodeposition should be approximately 7 cm · yr^{-1}, roughly 8 times the local burial rate calculated by Anderson *et al.* (1981). Using these same average values, an individual worm of 2 mg dry biomass would produce surface deposits at a rate of 90 cm^3 · y^{-1}, which is somewhat lower than the individual rates of *Clymenella torquata* (a larger worm) tabulated by Rhoads (1974).

b. Scoloplos abundance and bioadvective subduction velocity. The marker layer subduction experiment indicated that particle transport in incubation cores C7 and C8 was principally bioadvective. Marker particles moved predominately downward until they were injected back to the sediment surface after entering the *Scoloplos* feeding zone. As in similar experiments with *Tubifex tubifex* (Robbins *et al.*, 1979; Fisher *et al.*, 1980), marker peak broadening (eddy diffusion) did occur although its contribution to net particle distribution was obviously much less important than advective subduction. The enhanced peak broadening observed in core C8 near the end of the experiment was apparently due to the originally flat horizon becoming crenulated as it approached or entered the feeding zone. Assuming that this crenulation occurs because of nonhomogeneous distribution of actual sites of sediment reworking, the peak broadening observed here as well as in the tubificid experiment of Robbins *et al.* (1979) may actually be the result of lateral averaging of many localized advective "injections" or interfingerings of stratigraphically higher material to depth around conveyor-belt feeding sites.

The similarity of the core C7 : core C8 ratios of marker layer subduction velocities (4.3 : 1) and *Scoloplos* biomass densities (3.8 : 1) suggests that *Scoloplos* feeding and biodeposition could account for most of the reworking activity. Because the average porosity of core C8 was significantly greater than that of C7, taking porosity into account may bring these ratios into even better agreement. In fact, vertical variations in burial velocity in the sediment column are related fundamentally to the vertical distribution of pore space (Berner, 1980). To relate conveyor-belt faunal density and sediment processing rates to vertical transport below the sediment-water interface, the rather steep changes in porosity which characterize the upper bioturbated zone of muddy deposits must be taken into account.

Although the relationship between advective velocity of an infinitely thin horizon moving along the conveyor-belt, sediment porosity, and the density of conveyor-belt feeders may be determined by several methods, an approach analogous to the argument used by Berner (1980) to derive the steady-state compaction equation will be followed here. The one-dimensional diagenetic equation for a particulate substance m may be written as

$$\frac{\partial \hat{s}_m}{\partial t} = \frac{\partial}{\partial x}\left(D_B \frac{\partial \hat{s}_m}{\partial x} - \omega \hat{s}_m\right) + \Sigma Rxns \tag{2}$$

where:
x = depth measured positively downward from the sediment-water interface (always $x = 0$);
t = time;
$\hat{s}_m$ = concentration of particulate m per unit volume of wet sediment;
D_B = random mixing coefficient;
ω = advective velocity;
$\Sigma Rxns$ = rates of all processes producing or consuming particulate m.

Particle advective velocity is composed of an allochthonous burial component ω_i and a bioadvective (in the present case, conveyor-belt) component ω_B so that

$$\omega(x, t) = \omega_i(x, t) + \omega_B(x, t). \tag{3}$$

If all particulate tracer m is in the fine, ingestible fraction at a concentration s_m (e.g., moles tracer per gram ingestible particles) then

$$\hat{s}_m(x, t) = \rho[1 - \phi(x, t)]\, f(x, t)\, s_m(x, t) \tag{4}$$

where f = [mass ingestible particles]/[total particle mass] and ϕ = porosity. For a deposit containing only ingestible particles ($f = 1$) of constant average density ρ, Eq. 2 may be rewritten for the diagenesis of total solids ($s_m = 1$):

$$\frac{\partial}{\partial t}(1 - \phi) = \frac{\partial}{\partial x}\left(D_B \frac{\partial}{\partial x}(1 - \phi) - \omega[1 - \phi]\right) + \frac{1}{\rho}\Sigma Rxns. \tag{5}$$

Note that $1 - \phi$ is the volume of total solids in a unit volume of wet sediment ($cm^3 \cdot$ particles $\cdot\ cm^{-3}$). For present purposes, the only process contributing to the last term on the right-hand side of Eq. 2 is particle ingestion at depth by conveyor-belt feeders. Because effective biomass distribution (i.e., vertical distribution of biomass over all probable positions of the anterior end of the worms) controls the intensity of subsurface particle removal, we set

$$\Sigma Rxns = -\hat{B}(x, t)r(t) \tag{6}$$

where r is particle egestion rate as defined in Eq. 1 and $\hat{B}$ is the effective distribution of biomass (per unit volume) over the vertical feeding zone $\ell \leq x \leq L$ such that at any

time the standing crop of *Scoloplos* is

$$\bar{B} \equiv \int_{\ell}^{L} \hat{B}dx = \bar{B}\int_{\ell}^{L} \beta(x, t)dx = \bar{B}\int_{0}^{\infty} \beta(x, t)dx = \bar{B}\int_{-\infty}^{\infty} \beta(x, t)dx \tag{7}$$

where β is a (dimensionless) normalized distribution function with a value of zero outside of $\ell \leq x \leq L$. Assuming further that diffusive transport of particles and pore space is negligible (c.f., Berner, 1980), Eq. 5 may be rewritten as a compaction equation for bioadvective deposits:

$$\frac{\partial \phi}{\partial t} = \frac{\partial}{\partial x}(\omega(x, t)[1 - \phi(x, t)]) + \frac{\hat{B}(x, t)r(t)}{\rho} \tag{8}$$

Because particulates removed at depth are deposited at the sediment-water interface and surface porosity is essentially constant (0.80 to 0.83 near station 84-6), conservation of mass requires the surface boundary condition:

$$x = 0, \phi = \phi_0 = \text{constant}, \omega = \omega(0, t) = \omega_{i0}(t) + \omega_{B0}(t) \tag{9-a}$$

in which we assume (c.f., Eq. 1)

$$\omega_{B0}(t) \equiv \omega_B(0, t) = \frac{\bar{B}(t)r(t)}{\rho[1 - \phi_0]} \tag{9-b}$$

and $\omega_{i0}(t) = \omega_i(0, t)$. From Eqs. 8 and 9-a,b, the transient-state conveyor-belt velocity at any depth x is

$$\omega(x, t) = \frac{1}{1 - \phi(x, t)}\left[\omega_{i0}(t)[1 - \phi_0] + \int_0^x \frac{\partial \phi(\xi, t)}{\partial t} d\xi + \int_x^{\infty} \frac{\hat{B}(\xi, t)r(t)}{\rho} d\xi\right]. \tag{10}$$

For the special case where (1) $\bar{B}$ is constant with time, (2) rate of burial by newly deposited sediment ω_{i0} at the sediment-water interface does not vary with time, and (3) there are steady-state depth distributions of porosity and feeding sites, Eq. 10 reduces via Eq. 7 to

$$\omega(x, t) = \omega_{i0}\frac{1 - \phi_0}{1 - \phi(x)} + \frac{\bar{B}r(t)}{\rho[1 - \phi(x)]}\int_x^{\infty} \beta(x)dx \tag{11}$$

which, for r = constant is the steady-state compaction equation (Berner, 1980) corrected for biological removal of particles from depth to the surface. Assuming that β is a normalized Gaussian distribution function about $x = \bar{x}$ (the principle feeding depth) with standard deviation σ, then

$$\omega(x, t) = \omega_{i0}\frac{1 - \phi_0}{1 - \phi(x)} + \frac{\bar{B}r(t)}{2\rho[1 - \phi(x)]} erfc\left(\frac{x - \bar{x}}{\sigma\sqrt{2}}\right). \tag{12}$$

Values of *erfc*, the complement to the Gaussian error function, are tabulated in most

statistical handbooks; convenient closed-form approximations for use in computer subroutines are also available (e.g., Abramowitz and Stegun, 1970).

Eq. 12 is a useful predictor of advective velocity in deposits dominated by conveyor-belt type mixing in which (1) ω_{i0}, ρ, and $\bar{B}$ are constant, (2) all or nearly all particles are ingestible by conveyor-belt feeders, and (3) the assumption of steady-state porosity profile is valid and the extent of the feeding zone ($\ell = \bar{x} - 3\sigma \leq x \leq \bar{x} + 3\sigma = L$) can be estimated. Conceptually, ω can be considered to be the vertical (downward) velocity of any particle not ingested by the conveyor-belt feeder or of an imaginary, arbitrarily thin layer of material from which particles may be removed after the layer moves into the subsurface feeding zone. Although we will not do so here, one can easily show that the effects of several conveyor-belts operating at different rates about different principle feeding depths may be combined additively to produce bioadvection relationships similar to Eqs. 11 and 12. Regardless of the type of distribution required to describe the location of anterior ends, Eq. 11 demonstrates that conveyor-belt subduction of a horizon at any depth x is due to feeding activity occuring *below* that horizon, provided that the steady-state porosity profile is maintained. It is also clear that *conveyor-belt subduction of all particles is due to transport of those particles which the deposit-feeder selects for ingestion.*

Using this theoretical development, one can predict the depth-time relationships of marker horizons in cores C7 and C8, based only upon *Scoloplos* biodeposition after first calculating the corresponding depth profiles of bioadvective velocity. Assuming $\omega_{i0} = 0$ (no incoming sediment), $r = 120\ \text{g} \cdot \text{g}^{-1} \cdot \text{d}^{-1}$ (Table 2), $\rho = 2.7\ \text{g} \cdot \text{cm}^{-3}$, $\sigma = 0.5$ cm, and the following specific values for each core:

$$\text{C7: } \bar{B} = 1.202\ \text{g} \cdot \text{m}^{-2}, \qquad \bar{x} = 5\ \text{cm}, \phi(x) = 0.53 + 0.23 \exp(-0.423x)$$

$$\text{C8: } \bar{B} = 4.502\ \text{g} \cdot \text{m}^{-2}, \qquad \bar{x} = 6\ \text{cm}, \phi(x) = 0.34 + 0.46 \exp(-0.232x)$$

the velocity-depth profiles based on *Scoloplos* feeding and biodeposition were calculated (Fig. 6). The rapid drops in ω near the bottom of the profiles in Figure 6 occur within the *Scoloplos* feeding zone and are due to decreasing amount of feeding activity occurring below progressively deeper horizons. Mathematically, these rapid decreases arise from the behavior of the $erfc([x - \bar{x}]/\sigma\sqrt{2})$ function in the vicinity of $x = \bar{x}$; at $x \rightarrow {}^{-}\infty$ (i.e., shallower than $\bar{x} - 3\sigma$) *erfc* has a value of $+2$, at $x \rightarrow {}^{+}\infty$ (deeper than $\bar{x} + 3\sigma$) a value of 0, and from $\bar{x} - 3\sigma$ to $\bar{x} + 3\sigma$ *erfc* drops rapidly from 2 to 0 (inflection point at $x = \bar{x}$). In Figure 6 the slight deviations from the symmetrical rounded-z-shaped *erfc* curve are due to vertical changes in porosity (Eq. 12), especially in the top few cm.

The theoretical time lapse required for the burial of a marker layer to depth x was calculated as

$$\Delta t = \int_0^x \frac{d\xi}{\omega(\xi)}, \tag{13}$$

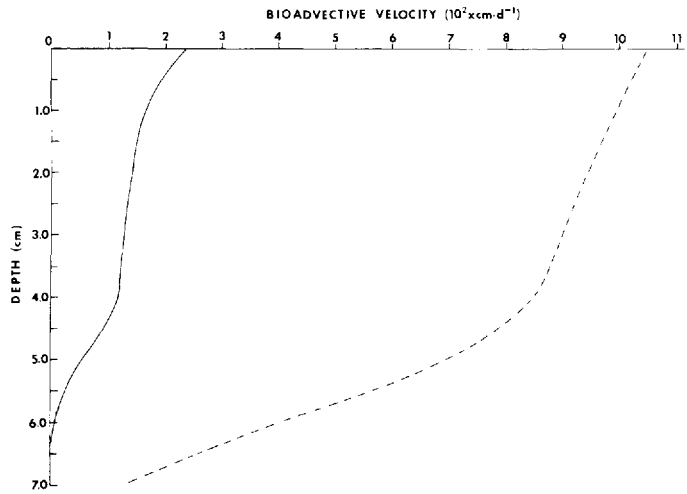

Figure 6. Bioadvective velocity of an infinitely thin sediment horizon due to conveyor-belt feeding by *Scoloplos* spp. in cores C7 (solid curves) and C8 (broken curve).

which agreed well with observed subduction patterns (Fig 5). In both cores, predicted depths during the first 50–60 days were slightly greater than those predicted from the velocity profiles of Figure 6. Because we used final biomasses to calculate these ω values and because there was probably some worm growth during the incubation (see above), this positive deviation during the first half of the experiment is not surprising. Because there was a normal, active macrofaunal community present throughout the experiment, these observations support the hypotheses that (1) *Scoloplos* spp. were the principle agents of bioturbation and that (2) the predominant mode of reworking was bioadvective.

c. Bioadvective contribution to sediment mixing in Lowes Cove. The Be-7 activity-depth distribution at station 84-6 may be used with certain assumptions to estimate the contribution of conveyor-belt feeding by *Scoloplos* spp. to *in situ* sediment turnover in Lowes Cove. As in the case of the incubation experiment, it is first necessary to develop conveyor-belt diagenetic equations to relate the Be-7 profile to observed biodeposition rates and abundance of the polychaetes. In so doing, we will assume that all of the Be-7 is bound to the fine sediment fraction, all of which is ingestible by *Scoloplos,* either as distinct particles or by entrainment in aggregates (Self and Jumars, 1978). We have observed that *Scoloplos* spp. from Lowes Cove ingest particles smaller than 250 μm (Rice *et al.,* 1986), consistent with other observations (Whitlatch, 1980). When erratic particles larger than 1 mm are removed from Lowes Cove sediment taken from the 0–10 cm depth range, at least 87% by weight of the remaining particulates are smaller than 250 μm (Rice *et al.,* 1986).

The one-dimensional general diagenetic equation (Eq. 2) for a radioactive tracer bound to particulates ingestible by a conveyor-belt feeder in a deposit undergoing only conveyor-belt bioadvective mixing is

$$\frac{\partial \hat{s}}{\partial t} = -\frac{\partial}{\partial x}(\omega \hat{s}) - \frac{\hat{B}(x, t) r(t)}{\rho[1 - \phi(x, t)]} \hat{s} - k\hat{s} \tag{14}$$

where $\hat{s}$ is the concentration of particulate tracer per unit volume of wet sediment, k is the radioactive decay constant, and all other terms are as described previously. Eq. 14 applies provided the tracer is distributed uniformly among particles and provided the deposit-feeder does not discriminate for or against particles bearing the tracer. As in Eqs. 8 and 9 above, conservation of tracer mass requires that tracer removed from depth and redeposited at $x = 0$ be accounted for in the formulation of the surface boundary condition (see Eqs. 23–26 below). Assuming ρ and f are constant, expanding the partial derivative on the right-hand side of Eq. 14, and using the mass-volume relationship in Eq. 4, Eq. 14 becomes

$$\frac{\partial s}{\partial t} = \frac{1}{1 - \phi}\left[\frac{\partial \phi}{\partial t} - \frac{\partial}{\partial x}(\omega[1 - \phi]) - \frac{\hat{B}r}{\rho}\right] s - \omega \frac{\partial s}{\partial x} - ks. \tag{15}$$

Concentrations s in Eq. 15 are now in *mass per unit mass of selectable particles* such that, as in Eq. 4,

$$\hat{s}(x, t) = \rho[1 - \phi(x, t)] f s(x, t). \tag{16}$$

At either transient- or steady state, the bracket terms on the right-hand side of 15 sum to zero (Eq. 8). Consequently, Eq. 15 reduces to the compact form

$$\frac{\partial s(x, t)}{\partial t} = -\omega(x, t) \frac{\partial s(x, t)}{\partial x} - ks(x, t). \tag{17}$$

A steady-state solution to this deceivingly simple bioadvective equation (the simplicity of Eq. 17 is offset by the complicated boundary conditions which will be discussed below) exists if the tracer nuclide concentration at the sediment surface and biodeposition rate are constant over time. A steady-state solution could also exist under fortuitous, but improbable, circumstances (see below). For the boundary condition

$$x = 0, \qquad s = s_0 = \text{constant} \tag{18}$$

the steady-state solution to Eq. 17 is

$$s(x) = s_0 \exp\left(-\int_0^x \frac{k d\xi}{\omega(\xi)}\right), \qquad \omega \neq \omega(t). \tag{19}$$

Transient-state solutions to Eq. 17 bear close resemblance to the steady-state solution. Although first-order problems are ordinarily solved as initial-value problems,

it is appropriate here to impose the time-dependent boundary condition

$$x = 0, \qquad s(0, t) = S_0(t) \tag{20}$$

where t is not restricted to positive values. This is in fact equivalent to a first-order initial-value problem in which the initial s vs x profile would be considered to have been generated by advection to depth of some historical surface condition $S_0(t<0)$. The transient-state solution to Eq. 17 subject to the constraint in Eq. 20 may be written in the convenient parametric form

$$s(x, t) = S_0(\tau)e^{-k[t-\tau]}, \qquad (\tau \leq t) \tag{21}$$

where τ is *stratigraphic time* (i.e., the historical time, relative to the zero of the t time scale, when a stratum at $x = x(t - \tau)$ was at the sediment surface) defined implicitly by the relation

$$x(t - \tau) = \int_{\tau}^{t} \omega(x, \theta)d\theta, \qquad (\tau \leq t). \tag{22}$$

It is important to bear in mind that t is the time of observation and that x and t are independent variables ($\partial x/\partial t = 0$). However, x does depend upon the time difference $t - \tau$. In practice, Eq. 22 may be used to generate ordered pairs of x and τ by numerical integration beginning at $\tau = t$, (the time of observation) and then decreasing τ in small decrements to calculate successive x, τ pairs, continuously correcting for porosity changes with depth.

The boundary conditions (Eqs. 18 and 20) are actually quite different from others commonly encountered in diagenetic theory. Considering that the natural boundary constraint is one of flux at the sediment surface, one must account for both new allochthonous material (with tracer concentration $s = s_{i0}$) and biodeposited material (with tracer concentration $\langle S_B \rangle$) which are introduced continually at $x = 0$; i.e., the flux *to* $x = 0$ is

$$J(0^-, t) = \omega_{i0}(t)s_{i0}(t) + \omega_{B0}(t)\langle s_B(t)\rangle. \tag{23}$$

The net flux *across* $x = 0$ is given by

$$J(0^+, t) = [\omega_{i0}(t) + \omega_{B0}(t)]S_0(t). \tag{24}$$

Because particles arriving at the sediment surface create ambient sediment surface (always defined as $x = 0$), these two fluxes are necessarily identical. Then, these flux constraints can also be expressed as the equivalent concentration boundary conditions of Eqs. 18 and 20; i.e.,

$$x = 0, \qquad S_0(t) = \frac{\omega_{i0}(t)s_{i0}(t) + \omega_{B0}(t)\langle s_B(t)\rangle}{\omega_{i0}(t) + \omega_{B0}(t)}. \tag{25}$$

Assuming for present purposes that the radionuclide tracer is not assimilated during passage through the deposit-feeder gut, a reasonable estimate of $\langle s_B \rangle$ is

$$\langle s_B(t) \rangle = \frac{\int_{\bar{x}-3\sigma}^{\bar{x}+3\sigma} s(\xi, t)\, \hat{B}(\xi)\, d\xi}{\int_{\bar{x}-3\sigma}^{\bar{x}+3\sigma} \hat{B}(\xi)\, d\xi} \tag{26}$$

since the contribution of particles from various depths to the surface biodeposit must be weighted according to the vertical feeding distribution of anterior ends in the deposit.

Eqs. 25 and 26 illustrate a fundamental property of conveyor-belt systems at transient and steady states: *the boundary condition at $x = 0$ is continuously dependent upon the internal solution of the transport-reaction problem.* In parallel work, B. P. Boudreau has developed the conveyor-belt diagenetic problem as a special case of "nonlocal mixing" (transport between nonadjacent points) (Boudreau, 1985; Boudreau, 1986). Interested readers are urged to consult his work, which also incorporates several hypothetical modes of random mixing into conveyor-belt models.

To examine the contribution of conveyor-belt feeding activity of *Scoloplos* spp. to the Be-7 activity-depth profile at station 84-6 (Table 4), one steady-state and four transient state solutions to Eq. 17 were used. The four transient-state solutions differ only in their inclusion or exclusion of time-varying atmospheric inputs of Be-7 to the sediment surface and seasonal (temperature-dependent) dilution of surface Be-7 by *Scoloplos* biodeposition. The general approach described below was to propagate the surface and/or topmost core section ($x = 0.0$–0.5 cm) Be-7 activity observed in July, 1984, to depth according to each transport model and compare results with the actual activity-depth profile. In all cases a steady-state porosity-depth profile (Table 4) was assumed.

i. Steady state: Constant biodeposition rate and constant surface concentration. In the simplest case, one might assume that biodeposition rate by *Scoloplos* and surface concentration of Be-7 remained constant. The assumption of constant surface concentration is not altogether unreasonable inasmuch as surface particle transport on the Lowes Cove flat is controlled by physical processes (Anderson *et al.*, 1981) which could buffer the surface particle chemistry. Also, because station 84-6 was sampled in early summer, the top few cm of the core, where Be-7 activity will undergo most of its decay, should represent material turnover occurring at year-average bioturbation rates (spring through early summer).

The steady-state conveyor-belt solution (Eq. 19) was used to predict the Be-7 activity-depth profile by projecting the surface ($x = 0$) and the topmost core section (0–0.5 cm, setting $x = 0.25$ cm) activities to depth. Advective velocity ω was calculated from Eq. 12 using values of $\omega_{i0} = 0.9$ cm · y^{-1}, $\bar{B} = 1.85$ g dry *Scoloplos* biomass · m^{-2}, $\bar{x} = 5.0$ cm, $\sigma = 0.5$ cm, and an annual-average $r = 60$ g dry sediment · g dry bio-

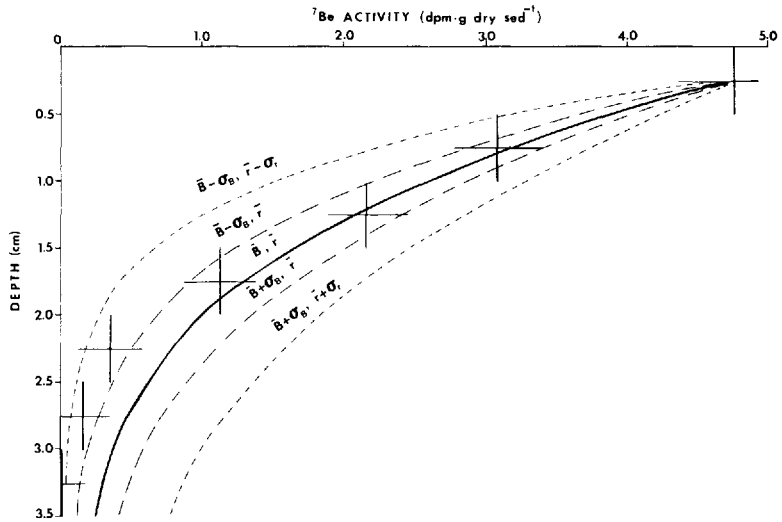

Figure 7. Be-7 depth profile at station 84-6 (July, 1986) and steady-state bioadvective profiles projected from $x = 0.25$ cm. The solid curve is the theoretical projection for an average *Scoloplos* standing crop of $B = 1.85$ g dry biomass · m^{-2} and year-averaged biodeposition rate $r = 60$ g dry sediment · g dry *Scoloplos*$^{-1}$ · d^{-1}. Other theoretical projections allowing for one standard deviation of uncertainty in average biomass ($\sigma_B = \pm 0.45$ g dry biomass · m^{-2}) and/or biodeposition rate ($\sigma_r = \pm 23$ g dry sediment · g dry Scoloplos^{-1} · d^{-1}) are indicated by the broken curves.

mass^{-1} · d^{-1}. For computational purposes, porosity data (Table 4) were represented by a continuous form $\phi(x) = 0.61 + 0.20 \exp(-0.72x)$ (Lerman, 1977).

The projection from $x = 0.25$ very nearly coincides with the actual data (Fig. 7), especially in the upper core intervals, which stratigraphically represent spring and early summer, 1984, biodepositional rates (see Fig. 10 below), which are close to the annual average biodeposition rate of $r = 60$ g · g^{-1} · d^{-1}. A decrease of one standard deviation in r and $\bar{B}$ (the latter is known with less certainty) improves the fit in the 1.5–2.5 cm depth range, which stratigraphically represents the winter months of late 1983–early 1984 (see Fig. 10) when both r and $\bar{B}$ should be below annual average values. The projection from $x = 0$ (not shown in Fig. 7) converges to the $x = 0.25$ cm projection in the 1.5–2.0 cm interval and differs markedly from the latter projection only in the 0–0.5 cm interval.

The Be-7 depth profile can also be used under steady-state assumptions to calculate an apparent random mixing coefficient for station 84-6. The equation commonly used assumes constant D_B and an average burial rate $\bar{\omega}_i$ (Berner, 1980):

$$D_B \frac{\partial^2 \hat{s}}{\partial x^2} - \bar{\omega}_i \frac{\partial \hat{s}}{\partial k} - k\hat{s} = 0. \tag{27}$$

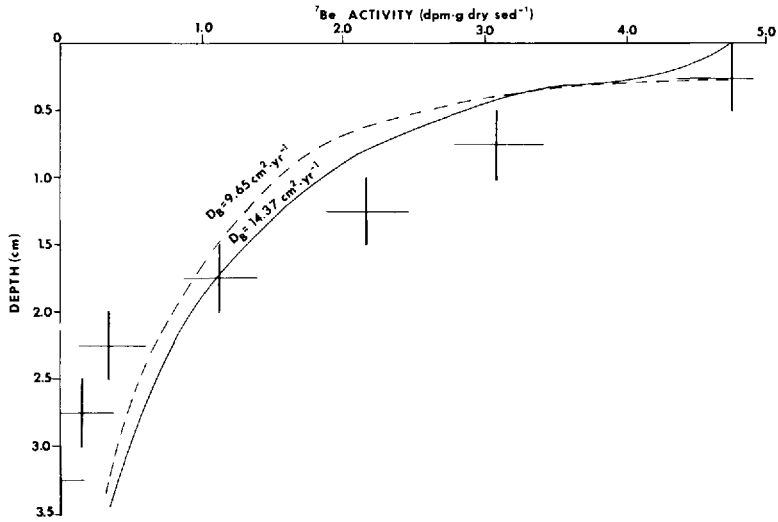

Figure 8. Curvefits of the usual random mixing model (Eq. 29) to the Be-7 depth profile at station 84-6 and calculated mixing coefficients. Estimations of D_B were made using both $x = 0$ and $x = 0.25$ cm as the upper boundary.

For present comparative purposes, appropriate boundary conditions are

$$x = 0, \qquad \hat{s} = \hat{s}_0; \tag{28-a}$$

$$x \longrightarrow \infty, \qquad \partial\hat{s}/\partial x \longrightarrow 0. \tag{28-b}$$

The well-known solution to Eqs. 27 and 28-a,b is

$$\hat{s}(x) = \hat{s}_0 e^{\lambda x} \tag{29}$$

where

$$\lambda = \frac{\overline{\omega}_i - \sqrt{\overline{\omega}_i^2 + 4kD_B}}{2D_B}. \tag{30}$$

For purposes of comparison, Eq. 29, written with Be-7 activity in dpm per unit volume of wet sediment, was converted to a dpm per unit mass dry sediment basis using Eq. 4 and fit to the Be-7 depth profile (Table 4, data from $x = 0$ to $x = 3.5$ cm) by nonlinear least-squares regression (Fig. 8). Best fits using both $x = 0$ and $x = 0.25$ cm as the upper boundary and a depth-averaged burial rate (i.e., corrected for porosity change with depth using the steady-state compaction equation (Berner, 1980)) of $\overline{\omega}_i = 0.5$ cm · y^{-1} were substantially inferior to those obtained with the steady-state conveyor-belt assumption (Fig. 7).

ii. Transient state: Case 1: Cyclic annual variation in biodeposition rate and constant Be-7 surface concentration. Given the rather special requirements for applicability of the steady-state assumption to the conveyor-belt diagenesis (Eqs. 18 and 19) and the argument presented above that surface concentration of Be-7 at Lowes Cove may be buffered hydrodynamically, one is left with the problems of determining (1) why the steady-state solution predicts the activity-depth profile so well and (2) if accounting for seasonal variations in conveyor-belt velocity can improve the predictions in Figure 7. If the Be-7 concentration at $x = 0$ is assumed to be buffered at some constant value, the transient state solution (Eqs. 21 and 22) will have a constant coefficient $S_0(\tau) = S_0$, and nonsteady concentrations at depth will arise solely as a result of time-dependent ω (Eq. 11). The activity-depth profile of the core from 84-6 can be predicted for such condition after obtaining a functional estimate of seasonal (time, temperature) dependence of biodeposition rate.

Assuming that biomass-specific biodeposition rate r is a function of temperature only and that laboratory determinations of r may be extrapolated to the field, then the r *vs* temperature data of Rice *et al.* (1986) discussed above may be used to estimate seasonal variations in biodeposition by *Scoloplos* in Lowes Cove. Local records indicate that seawater temperature at the Cove mouth varies approximately sinusoidally between a maximum of about 21°C in mid-August and a low around 0°C in mid-February. Setting the zero of time as 1 January, 1984, absolute temperature T variation of Lowes Cove may be approximated by

$$T(t) = T_1 + \frac{1}{2} T_2 \left[1 - \cos\left(\frac{2\pi t}{P} - \frac{\pi}{4}\right)\right] \tag{31}$$

where T_1 = minimum annual temperature (273.15°K) assumed to fall in the middle of February (⅛ year after $t = 0$ (1 January) or $\pi/4$ radians in a cycle of 2π radians); T_2 = difference between maximum and minimum temperatures (21°C − 0°C = 21°); and P = annual period of 365.25 days. To calculate seasonal biodeposition rates, Eq. 31 may be substituted into the Arrhenius equation

$$r(T) = Ae^{-E_a/RT(t)} \tag{32}$$

where $A = 1.39 \times 10^{22}$ g · g^{-1} · d^{-1}, $E_a = 27.0$ kcal · mol^{-1}, and $R = 1.987 \times 10^{-3}$ kcal · deg^{-1} · mol^{-1} (Rice *et al.*, 1986). As mentioned earlier, however, the Arrhenius relationship tends to underestimate r at lower temperatures. A more realistic representation, achieved by setting $T_1 = 283$°K, is shown in the inset to Figure 9.

Holding S_0 constant and allowing ω to vary seasonally with temperature improved the prediction of the Be-7 activity-depth profile, especially in the 1.5 to 3.5 cm range (Fig. 9). The predicted profile was determined from Eqs. 21 and 22 with $S_0 = 4.62$ dpm · g^{-1} (Table 4) and at observation time $t = 190$ days (8 July, 1984, with $t = 0$

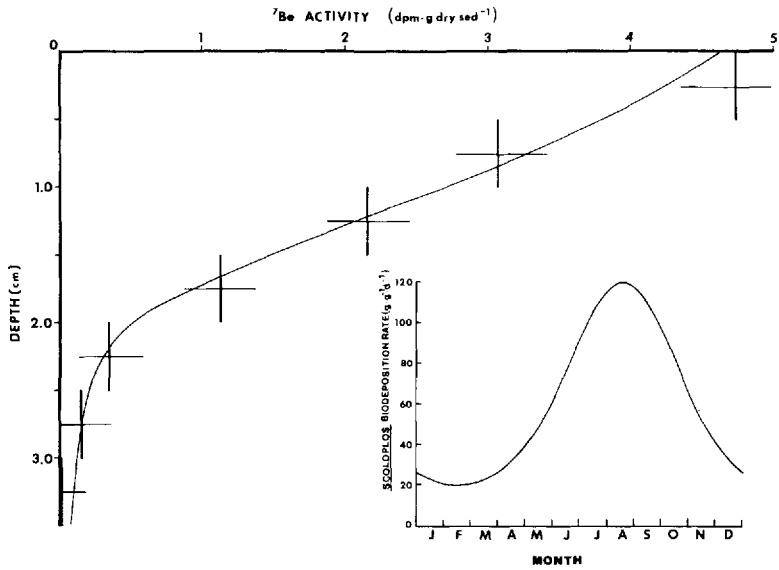

Figure 9. Be-7 depth profile at station 84-6 and theoretical transient-state profile generated by assuming a constant surface concentration (4.62 dpm · g^{-1}) and time-varying biodeposition rate by *Scoloplos* (inset illustration).

defined as 1 January, 1984). Time-dependent advective velocity (Eq. 12) was calculated from the cyclic time-temperature relations of Eqs. 31 and 32 using the same values of ω_{i0}, $\phi = \phi(x)$, $\overline{B}$, σ, and $\overline{x}$ as in the steady-state calculation. Comparing this result (Fig. 9) with the steady-state prediction (Fig. 7) indicates, not surprisingly, that time-dependent variations in conveyor-belt velocity prior to July, 1984, substantially influenced the subsurface Be-7 profile actually found. Nevertheless, it is still clear that the steady-state prediction is in remarkably good agreement with the data and with this transient-state prediction.

If one accepts for the moment that constant Be-7 surface concentration is maintained (this will be considered again below) and that sediment turnover at 84-6 is controlled by *Scoloplos* feeding activity, this agreement is fairly easy to understand. The time-stratigraphic relationship for the sediments calculated from Eqs. 12 and 22, based only upon *Scoloplos* biodeposition (with the same parameter values used to calculate the theoretical profile of Fig. 9), indicates that most (ca. 70%) of the top 5 cm of sediment at 84-6 was turned over during preceding warm months (spring through autumn 1983, and late spring through early summer of 1984) (Fig. 10). During these months the average biodeposition rate should be very close to the value of 60 g · g^{-1} · d^{-1} used in the steady-state prediction (Fig. 7). Consequently, if the constant boundary concentration at $x = 0$ is accepted, the predictive success of the steady-state model is not surprising.

iii. Transient state: Cyclic annual variation in biodeposition rate with variable Be-7 surface concentration due to variations in atmospheric deposition and/or conveyor-belt dilution. The conveyor-belt boundary condition (Eq. 25) required by mass balance indicates that surface concentration of a tracer such as Be-7 is dependent upon tracer concentrations in new allochthonous particles and in recycled particles and upon surface allochthonous burial and bioadvective velocities. Clearly, S_0 may be constant only (1) if the concentrations in new and recycled material change seasonally in such a way as to perfectly balance varying ω or (2) if the boundary condition is ineffective because of external buffering. This observation brings into question the assumption used above that the surface concentration was constant, especially when one considers that atmospheric depositional flux of Be-7 to the earth's surface varies significantly over the year (Turekian *et al.*, 1983). Therefore, three other hypothetical transient-state cases were considered. In each of these ω was considered to vary cyclically as in Case 1, and $S_0(\tau)$ was allowed to vary such that:

Case 2: $S_0(t)$ is determined only by atmospheric depositional flux of Be-7 ($s_{i0}(t)$ is proportional to flux) and conveyor-belt dilution is ineffective; then for constant ω_{i0},

$$S_0(\tau) = \frac{J_{\text{atm}}(t)}{J_{\text{atm}}(190)} S_0(190); \tag{33}$$

Case 3: $S_0(t)$ is determined only by variable conveyor-belt dilution with dead sediment (s_{i0} must necessarily be constant); then for constant ω_{i0},

$$S_0(\tau) = \frac{\omega_{i0} + \omega_{B_0}(190)}{\omega_{i0} + \omega_{B0}(t)} S_0(190); \tag{34}$$

Case 3: $S_0(t)$ is determined by the combined effects of variable atmospheric deposition and conveyor-belt dilution; then for constant ω_{i0},

$$S_0(\tau) = \frac{J_{\text{atm}}(t)}{J_{\text{atm}}(190)} \frac{\omega_{i0} + \omega_{B0}(190)}{\omega_{i0} + \omega_{B_0}(t)} S_0(190). \tag{35}$$

Boundary constraints 33, 34, and 35 follow directly from the general conveyor-belt boundary condition (Eq. 25) because the *Scoloplos* feeding zone is deeper than the zone of continuously (with depth) detectable Be-7 activity (Fig. 10). That is, for $\langle s_B \rangle = 0$, the general boundary constraint for Be-7 at station 84-6 was taken to be

$$S_0(t) = s_{i0}(t) \frac{\omega_{i0}}{\omega_{i0} + \omega_{B0}(t)}. \tag{36}$$

Boundary constraints 33 derives from the very reasonable assumption that any particles present in atmospheric percipitation do not themselves contribute to surface burial ω_{i0}; however, the deposited Be-7 may become associated with water-transported

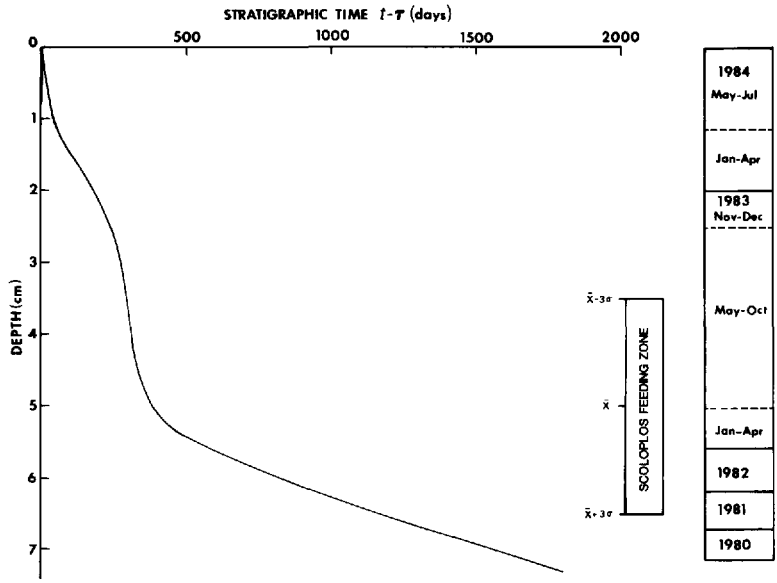

Figure 10. Time-stratigraphic relationships at station 84-1 (July, 1984) assuming B = 1.85 g dry *Scoloplos* · m^{-2} and time-varying *Scoloplos* biodeposition rate (see inset, Fig. 9).

or suspension-feeder-transported particles that do contribute to ω_{i0}. Then for ω_{i0} = constant, Eq. 33 follows immediately. For boundary constraint 34 to apply, s_{i0} must be constant, and the flux across $x = 0$ must be constant over time. This constancy of flux follows necessarily because as advective velocity increases or decreases, $S_0(t)$ will decrease or increase proportionally because of conveyor-belt dilution.

The transient-state activity-depth projections were made for Cases 2, 3, and 4 using the same solutions and parameter values as for transient-state Case 1, except that the variable boundary constraints above (33, 34, and 35) were applied. To estimate the effect of variable atmospheric depositional flux of Be-7 (Cases 2 and 4), relative fluxes $(J_{atm}(t)/J_{atm}(190))$ were calculated assuming that atmospheric depositional flux of this nuclide on any given day of a month between May, 1983, and June, 1984, was proportional to total wet precipitation during that month (Turekian *et al.*, 1983) in the nearby town of Newcastle, Maine (Table 5). June, 1984, was chosen as the base period for calculating the atmospheric depositional ratios because the time of sampling (t = 190 days) was only about 1 week into July, 1984. Although this is obviously only an approximation, it seems to be a reasonable one for an intertidal to shallow subtidal environment in direct or nearly direct contact with the atmosphere.

The actual Be-7 in core sections from 84-6 are compared to predicted transient-state interval-averaged activities in Table 6. To facilitate comparison with the activities in core sections (Table 4), the transient-state predictions were averaged over depth

Table 5. Monthly precipitation at Newcastle, Maine, from May, 1983 through July, 1984.*

Date	Precipitation (cm)	Normalized**	Date	Precipitation (cm)	Normalized**	Date	Precipitation (cm)	Normalized**
1983 May	15.2	10.9	1983 Oct	7.7	0.55	1984 Mar	17.2	1.23
Jun	3.1	0.22	Nov	36.3	2.59	Apr	9.7	0.69
Jul	6.3	0.45	Dec	23.6	1.69	May	22.5	1.61
Aug	8.4	0.60	1984 Jan	7.7	0.55	Jun	14.0	1.00**
Sep	3.7	0.26	Feb	15.9	1.14	Jul	8.0	(1.00)***

*Precipitation data source: National Oceanic and Atmospheric Administration, Northeast Regional Climate Center. 1983, 1984. Maine Climate.

**Normalized relative to total precipitation of June, 1984.

***July, 1984, precipitation through time of sampling (8 July) assumed to be characterized better by the June, 1984, level.

Table 6. Comparison of actual Be-7 depth profiles at station 84–6 (August, 1981) with interval-averaged predictions from four transient-state diagenetic models based on conveyor-belt transport by *Scoloplos:* (1) variable feeding rate and constant surface concentration; (2) variable feeding rate and variable surface concentration due only to monthly variation in atmospheric deposition of Be-7 by precipitation; (3) variable feeding rate and variable surface concentration due only to differential dilution of surface Be-7 by time-dependent biodeposition of "dead" sediment from depth; and (4) variable feeding rate and variable surface concentration due to the combined effects of time-dependent atmospheric input and biogenic dilution by "dead" sediment. Be-7 concentrations are given as specific activity (dpm · g dry sediment^{-1}).

			Time-Dependent Surface Concentration		
Depth Interval (cm)	Data (Table 4)	Constant Surface Concentration (Case 1)	Due to variable atmospheric flux only (Case 2)	Due to variable conveyor-belt dilution only (Case 3)	Due to biol. dilution & atmosph. flux (Case 4)
Surface	4.62	4.62	4.62	4.62	4.62
0.0–0.5	4.76	4.17	4.17	4.48	4.48
0.5–1.0	3.08	3.20	3.49	4.35	4.82
1.0–1.5	2.16	2.08	2.87	4.42	5.69
1.5–2.0	1.12	0.94	0.85	3.27	3.01
2.0–2.5	0.35	0.33	0.46	0.99	1.21
2.5–3.0	0.15	0.17	0.24	0.27	0.41
3.0–3.5	0	0.12	0.04	0.12	0.03

intervals corresponding to actual sampling intervals $x_1 \leq x \leq x_2$ (c.f., Aller, 1980) using the relationship

$$\begin{matrix} s(x, 190) \\ \text{Averaged over the} \\ \text{interval } x_1 \leq x \leq x_2 \end{matrix} = \frac{\int_{x_1}^{x_2} s(x, 190)\,[1 - \phi(x)]\,dx}{\int_{x_1}^{x_2} [1 - \phi(x)]\,dx}. \tag{37}$$

Assuming constant surface concentration and variable feeding rate (Case 1) produced the best overall agreement (c.f., Fig. 9), the major disagreement occurring in the topmost interval. Allowing the Be-7 activity in newly deposited material to vary with monthly precipitation and ignoring any conveyor-belt effect on surface Be-7 activity (Case 2) also produced good agreement, although not as good as with Case 1. Whether one assumes that variable atmospheric input affects the surface activity or not (Cases 3 and 4), assuming that time-dependent conveyor-belt velocity effected surface activity generally led to overestimated activities at depth. However, the variable conveyor-belt dilution effect did improve agreement in the 0–0.5 cm interval.

The calculations and comparisons in Table 6 are consistent with the hypothesis that the Be-7 surface activity in Lowes Cove is controlled predominately by external geophysical factors rather than conveyor-belt dynamics. Although all evidence points

to conveyor-belt dynamics driven by *Scoloplos* as the major control on subsurface particle transport in the top several cm, the hypothetical conveyor-belt boundary condition appears to be so strongly controlled externally as to be almost ineffective in influencing $S_0(t)$. Comparison of the results of Cases 1 and 2 suggests that variations in atmospheric input are also buffered, but not by conveyor-belt dilution (Case 4). Conversely, in the topmost core interval (0–0.5 cm), which stratigraphically represents late May to early July, 1984, allowing for differential conveyor-belt dilution brings model and data into agreement which could not be obtained otherwise. It is reasonable to expect this positive influence here (1) because rising temperature causes feeding rate to increase sharply in late Spring (Figs. 9 and 10) and (2) because the Cove is sedimentologically and hydrologically quiescent during these warmer months (Anderson *et al.*, 1981) so that biological effects may be more apparent.

The direct and indirect evidence presented above also suggests that the *apparent* steady-state Be-7 profile found at 84-6 arose from the combined effects of external buffering of surface Be-7 activity and the predominance of advective sediment turnover by *Scoloplos* during the spring to autumn period. If most of the Be-7 arriving at the sediment surface is retained in dispersed clay-size and smaller particles, Be-7 may actually be winnowed out of the slits of Lowes Cove by shallow-water waves and currents which control lateral dispersion on the flat (Anderson *et al.*, 1981). The possibility that surface trapping and retention of Be-7-rich fine particulates are controlled by microtopographic features, epibenthic microbial exudates, and suspension feeding activity cannot be dismissed (Rhoads and Boyer, 1982). Between-grain scale microtopography provides a nearly constant concentration of epibenthic traps for subsilt fines and might most easily account for a steady-state Be-7 surface activity in Lowes Cove. Further work at other stations in Lowes Cove characterized by other macrobenthic assemblages and different abundances of *Scoloplos* indicate that the macrofaunal and diagenetic associations we have reported here for station 84-6 are not serendipitous (Bembia, 1985).

d. Relationships between the abundance of Scoloplos and other benthic biogeochemical phenomena. Subsurface transport phenomena and the geochemical evolution of sedimentary deposits are inextricably related (Berner, 1980; Aller, 1980, 1982). In particular, the intensity of sediment reworking exerts a major control on the incorporation of material on the sediment surface into the deposit. Whether biological mixing is random or advective, increasing abundances of key macrofauna and higher individual reworking rates result in higher standing amounts of reactive allochthonous surface material in the subsurface deposit creating benthic geochemical "hotspots" in patches of high faunal density (Aller, 1982).

In Lowes Cove, the intensity of a number of biogeochemical properties is associated with the abundance of *Scoloplos* spp. There is a very tight positive correlation between the standing corp of *Scoloplos* and depth-average concentration of particulate organic

matter (POM) (Rice and Whitlow, 1985b). Considering (1) that the year-averaged concentration of POM on the sediment surface of the Cove varies only slightly (Mayer *et al.*, 1985) and (2) that decomposing particulate organic detritus derived from algal sources typically has an apparent first-order decay constant similar to that of Be-7 (Rice and Tenore, 1981), we expect concentration-depth profiles of the easily-decomposed fraction of sedimentary POM to resemble those of Be-7 at various conveyor-belt velocities corresponding to different abundances of *Scoloplos*. That is, for constant surface concentration, at high $k/\overline{B}$ ratios the POM or radionuclide depth-profile in the conveyor-belt zone should attenuate rapidly and at progressively lower $k/\overline{B}$ ratios the profile should approach the vertical (c.f., Aller's (1982) analog with randomly-mixed deposits). Both in theory and in fact, increasing concentrations of labile organic matter are found in the bioturbated zone of Lowes Cove sediment patches inhabited by greater abundances of *Scoloplos* (Rice and Whitlow, 1985a,b).

The maintenance of characteristic *Scoloplos* patch density on a seasonal and yearly basis (Fig. 4) may be due in part to population-level control of subduction of food resources. For a given surface concentration of POM, higher-density patches of *Scoloplos* should subduct proportionally higher amounts of potential food resources into the subsurface feeding zone. Moreover, a greater fraction of the easily decomposed (and consequently, more assimilable; Tenore and Rice, 1980) fraction of surface organic matter should be preserved for use by subsurface feeders. Dense patches of *Scoloplos* and presumably of other established assemblages of conveyor-belt deposit-feeders are then, in a sense, self-sustaining. In Lowes Cove and other marine environments where surface concentrations of organic matter are approximately buffered over time, physically distinct patches of subsurface deposit-feeders may then compete with one another, with patch or population density being a primary determinant of competitive success (Aller, 1982). For a given conveyor-belt species or set of species occupying similar feeding niches in some locality, the conveyor-belt feeding habit may represent, among other things, a population density-dependent adaptation to ameliorate intra- and interspecific competition for food resources.

Faunal density-dependent control upon sediment mixing and upon some diagenetic processes may have other feedback implications for the biochemistry of individual worms. Concentrations of ammonium acetate-extractable Cu, Zn, Cd, and Ag in shallow sediments at Lowes Cove and total concentrations of these trace metals in *Scoloplos* are inversely related to *Scoloplos* patch density (Rice and Whitlow, 1985a,b). These patterns may be related to observed increases in rates of metal solubilization (as organic complexes?) near the sediment surface and increased rates of fixation into refractory phases (sulfides?) near the RPD that are found at higher abundances of *Scoloplos* (Rice and Whitlow, 1985b). Inasmuch as these trace metal biogeochemical patterns are attributable to differences in the rates of subduction of labile POM across the sediment surface, they are reminiscent of the lower trace metal concentrations found in larger populations of *Capitella capitata* supported by proportionally greater experimental input rations of organic detritus (Rice *et al.*, 1982).

The density-dependent control of sediment turnover and early diagenesis demonstrated in the Lowes Cove system should be apparent in other benthic environments in middle to late stage succession, but sedimentological and hydrodynamic differences must be borne in mind. In many deep water environments wave and current activity is not as likely to influence conditions at the sediment surface strongly; thus, seasonal variation of inputs of allochthonous material and conveyor-belt dilution are more likely to produce time-dependent conveyor-belt boundary conditions (Boudreau, 1986). Also, because *Scoloplos* spp. and many other conveyor-belt macrofauna which feed on fine particles also thrive in sediments containing a large fraction of noningestible particles, the assumption that $f = 1$ (see Eq. 4) and calculations on that basis of must be considered carefully. J. A. Robbins has recently developed a particle-selective conveyor-belt transport model that should prove useful in the study of such sediments (Robbins, 1986). In extreme cases, such as Cape Henlopen, Delaware, where *Scoloplos fragilis* lives in fairly well-sorted coarse sand (Brown, 1982), the conveyor-belt phenomenon almost certainly does not even exist. Although *S. fragilis* at Cape Henlopen does egest fine material upon the surface (largely diatomaceous material (B. Brown and T. S. Bianchi, personal communications)), any initial or return flow of fine particles to depth is probably due to sinking through a more or less fixed framework of sand and gravel or to physical disturbance.

5. Conclusions

Biological reworking of the top 4–7 cm of sediment in Lowes Cove, Maine is controlled primarily by the conveyor-belt feeding and biodeposition activities of *Scoloplos* spp. The mode of particle transport is distinctly bioadvective, random mixing being of far less importance.

The Be-7 profile of a core taken from Lowes Cove in July, 1984, may be described by a simple steady-state bioadvective diagenetic model based solely upon the feeding rate of *Scoloplos* spp. and a constant surface concentration of Be-7. Allowing *Scoloplos* biodeposition rate to vary with the annual temperature cycle significantly improved the prediction of the Be-7 concentration-depth profile.

Accounting for seasonal variations in atmospheric deposition of Be-7 and dilution of Be-7 on the sediment surface by conveyor-belt dilution—a necessary consequence of the conveyor-belt boundary condition demanded for mass balance—generally did not improve upon a diagenetic model in which the surface Be-7 concentration was considered to be time-invariant, suggesting that the surface concentration was externally buffered by physical processes. Dilution of surface concentrations by biodeposited material from depth may be more important during warmer parts of the year when physical disturbances by currents and waves are minimal and conveyor-belt feeding activity is maximal.

Patches of conveyor-belt feeders may persist at self-sustaining densities when they are present in sufficient numbers to control sediment turnover in general and the

subduction of organic detritus in particular. Under such circumstances, these deposit-feeders may exert major controls upon both the overall subsurface transport properties and the chemical evolution of the deposit.

Acknowledgments. I thank T. S. Bianchi, E. G. Roper, and S. I. Whitlow for their indispensible help in the field and laboratory. P. Bembia helped in the field in 1984 and also carried out the Be-7 determinations. J. Barbaro also assisted in the field and provided the porosity data for core 84-6. A. Hillyard, L. Mayer, M. Musick, and L. Watling kindly accommodated us with field laboratory space and logistic support at the I. C. Darling Center, University of Maine at Orono.

This paper has benefitted greatly from the critical reviews of several scientists, particularly Drs. R. C. Aller, B. P. Boudreau, and L. M. Mayer. I especially thank Prof. D. C. Rhoads for the many delightful discussions during which he shared with me his insights and speculations on the conveyor-belt phenomenon.

Research funding was provided by a postdoctoral fellowship from the National Oceanic and Atmospheric Administration (NA81AA-D-00099) and National Science Foundation grant numbers OCE-8310178 and OCE-8442759. Contribution number 178 from the I. C. Darling Center, University of Maine at Orono.

This paper is dedicated to the memory of my father, L. C. Rice, who passed away shortly before this project began in July, 1981.

REFERENCES

Abramowitz, M. and I. A. Stegun. 1970. Handbook of Mathematical Functions with Formulas, Graphs, and Mathematical Tables. Dover Publ., NY, 1046 pp.

Aller, R. C. 1980. Diagenetic processes near the sediment-water interface of Long Island Sound. I. Decomposition and nutrient element geochemistry (S, N, P). Adv. Geophys., *22,* 237–350.

—— 1982. The effects of macrobenthos on chemical properties of marine sediment and overlying water, *in* Animal-Sediment Relations, P. L. McCall and M. J. S. Tevesz, eds., Plenum Press, NY, 53–102.

Aller, R. C. and J. K. Cochran. 1976. Th-234/U-238 disequilibrium in nearshore sediment: particle reworking and diagenetic time scales. Earth Planet. Sci. Lett., *20,* 37–50.

Aller, R. C. and R. E. Dodge. 1974. Animal-sediment relations in a tropical lagoon, Discovery Bay, Jamacia. J. Mar. Res., *32,* 209–232.

Anderson, F. E., L. Black, L. E. Watling, W. Mook and L. M. Mayer. 1981. A temporal and spatial study of mudflat erosion and deposition. J. Sed. Pet., *51,* 729–736.

Bembia, P. J. 1985. Bioadvective sediment mixing and beryllium-7 diagenesis in intertidal sediments, Lowes Cove, Maine, M. A. thesis, State University of New York, Binghamton, NY, 61 pp.

Berner, R. A. 1980. Early Diagenesis. Princeton Univ. Press, Princeton, NJ, 214 pp.

Boudreau, B. P. 1985. Diagenetic models of biological processes in aquatic sediments. Ph.D. dissertation, Yale University, New Haven, CT, 526 pp.

—— 1986. Mathematics of tracer mixing in sediments: II. Nonlocal mixing and the biological conveyor-belt phenomenon. Am. J. Sci., *286,* 199–238.

Brown, B. 1982. Spatial and temporal distribution of a deposit-feeding polychaete on a heterogeneous tidal flat. J. Exp. Mar. Biol. Ecol., *65,* 213–267.

Fisher, J. B. 1982. Effects of macrobenthos on the chemical properties of freshwater sediments, *in* Animal-Sediment Relations, P. L. McCall and M. J. S. Tevesz, eds., Plenum Press, NY, 117–220.

Fisher, J. B., W. J. Lick, P. L. McCall and J. A. Robbins. 1980. Vertical mixing of lake sediments by tubuficid oligochaetes. J. Geophys. Res., *85,* 3997–4006.

Goldberg, E. D. and M. Koide. 1962. Geochronological studies of deep sea sediments by the ionium/thorium method. Geochim. Cosmochim. Acta, *26,* 417–450.

Guinasso, N. L. and D. R. Schink. 1975. Quantitative estimates of biological mixing rates in abyssal sediments. J. Geophys. Res., *80,* 3032–3043.

Johnson, R. G. 1971. Animal-sediment relations in shallow water benthic communities. Mar. Geol., *11,* 93–104.

Krishnaswami, S., L. K. Benninger, R. C. Aller and K. L. Von Damm. 1980. Atmospherically-derived radionuclides as tracers of sediment mixing and accumulation in nearshore marine and lake sediments: evidence from Be-7, Pb-210, and Pu-239,240. Earth Planet. Sci. Lett., *47,* 307–318.

Krishnaswami, S., M. C. Monaghan, J. T. Westrich, J. T. Bennett and K. K. Turekian. 1984. Chronologies of sedimentary processes in sediments of the FOAM site, Long Island Sound, Connecticut. Am. J. Sci., *284,* 706–733.

Larsen, I. L. and N. H. Cutshall. 1981. Direct determination of Be-7 in sediments. Earth Planet. Sci. Lett., *54,* 379–384.

Lerman, A. 1977. Migrational processes and chemical reactions in interstitial waters, *in* The Sea, Vol. 6, E. D. Goldberg, I. N. McCave, J. J. O'Brien and J. H. Steele, eds., Wiley-Interscience, NY, 695–738.

Mayer, L. M., P. T. Rahaim, W. Guerin, S. A. Macko, L. Watling and F. E. Anderson. 1985. Biological and granulometric controls on sedimentary organic matter of an intertidal mudflat. Estuar. Coastal Shelf Sci., *20,* 491–503.

McCall, P. L. and J. B. Fisher, 1980. Effects of tubificid oligochaetes on physical and chemical properties of Lake Erie sediments, *in* Aquatic Oligochaete Biology, R. O. Brinkhurst and D. G. Cook, eds., Plenum Press, NY, 253–317.

McCall, P. L. and M. J. S. Tevesz. 1982. The effects of benthos on physical properties of freshwater sediments, *in* Animal-Sediment Relations, P. L. McCall and M. J. S. Tevesz, eds., Plenum Press, NY, 105–176.

Meyers, A. C. 1977a. Sediment processing in a marine subtidal sandy community. I. Physical aspects. J. Mar. Res., *35,* 609–632.

—— 1977b. Sediment processing in a marine subtidal sandy community. II. Biological aspects. J. Mar. Res., *35,* 633–647.

Nozaki, Y., J. K. Cochran, K. K. Turekian and G. Keller, 1977. Radiocarbon and Pb-210 distribution in submersible-taken deep sea cores from Project FAMOUS. Earth Planet. Sci. Lett., *36,* 167–173.

Rhoads, D. C. 1974. Organism-sediment relations on the muddy sea floor, *in* Oceanogr. Mar. Biol. Ann. Rev., *12,* 263–300.

Rhoads, D. C. and L. F. Boyer. 1982. The effects of marine benthos on physical properties of sediments: a successional perspective, *in* Animal-Sediment Relations, P. L. McCall and M. J. S. Tevesz, eds., Plenum Press, NY, 3–52.

Rice, D. L., T. S. Bianchi and E. H. Roper. 1986. Experimental studies of sediment reworking and growth of *Scoloplos* spp. (Orbiniidae: Polychaeta). Mar. Ecol. Prog. Ser., (in press).

Rice, D. L. and K. R. Tenore. 1981. Dynamics of carbon and nitrogen during the decomposition of detritus derived from estuarine macrophytes. Estuar. Coastal Shelf Sci., *13,* 681–690.

Rice, D. L., K. R. Tenore and H. L. Windom. 1982. Effect of detritus ration on metal transfer to deposit-feeding benthos. Mar. Ecol. Prog. Ser., *5,* 135–140.

Rice, D. L. and S. I. Whitlow. 1985a. Early diagenesis of transition metals: a study of metal partitioning between macrofaunal populations and shallow sediments, *in* The Fate and Effects

of Pollutants, Proceedings of a Maryland Seagrant Symposium, Maryland Seagrant Office, 21–30.

—— 1985b. Diagenesis of transition metals in bioadvective marine sediments, *in* Heavy Metals in the Environment, Vol. 2, T. D. Lekkas, ed., C. E. C. Consultants Ltd., Edinburgh, 353–355.

Robbins, J. A. 1986. A model for particle-selective transport of tracers in sediments with conveyor-belt deposit-feeders. J. Geophys. Res., (in press).

Robbins, J. A., P. L. McCall, J. B. Fisher and J. R. Krezoski. 1979. Effect of deposit-feeders on migration of Cs-137 in lake sediments. Earth Planet. Sci. Lett., *42,* 277–287.

Self, R. and P. A. Jumars. 1978. New resource axes for deposit feeders. J. Mar. Res., *36,* 627–641.

Tenore, K. R. and D. L. Rice. 1980. A review of trophic factors affecting secondary production of deposit-feeders, *in* Marine Benthic Dynamics, K. R. Tenore and B. C. Coull, eds., Univ. of South Carolina Press, Columbia, SC, 325–340.

Turekian, K. K., L. K. Benninger and E. P. Dion. 1983. Be-7 and Pb-210 total deposition fluxes at New Haven, Connecticut and at Bermuda. J. Geophys. Res., *88,* 5411–5419.

Wachs, B. 1967. Die Oligochaeten-Fauna der Fleissgewasser unter besonderer Berucksichtigung der Beziehungen zwischen der Tubificiden-Besiedlung und dem Substrat. Arch. Hydrobiol., *63,* 310–386.

Whitlatch, R. B. 1980. Patterns of resource utilization and coexistence in marine intertidal deposit-feeding communities. J. Mar. Res., *38,* 743–765.

Received: *14 August, 1985;* revised: *5 November, 1985.*